



## An Investigation into the Behavior of Disc Brake Wear

Dr. Aziz Al-Alawi    Dr. Albert E. Yousif    Muneer A. H. Jassim

*Mechanical Engineering Department*

*college of Engineering*

*University of Baghdad*

(Received 22 January 2007; accepted 5 March 2007)

### Abstract:

A reliable method of predicting brake pad wear, could lead to substantial economies of time and money. This paper describes how such a procedure has been used and gives the results to establish its reliability by comparing the predicted wear with that which actually occurs in an existing service.

The experimental work was carried out on three different commercial samples, tested under different operational conditions (speed, load, time ... etc) using a test rig especially modified for this purpose.

Abrasive wear is mainly studied, since it is the type of wear that takes place in such arrangements. Samples were tested in presences of sand or mud between the mating surfaces under different operational conditions of speed, load and braking time.

Mechanical properties of the pad material samples (hardness, young's modulus and collapse load under pure bending condition) were established. The thermal conductivity and surface roughness of the pad material were also found in order to enable comparison between the surface condition before and after testing.

Sliding velocity had a small effect on the wear rate but it had great effect on friction coefficient. Wear rate was affected mainly by the surface temperature which causing a reduction in friction coefficient and increasing the wear rate. Surface roughness had almost no effect on the wear rate since it was proved experimentally, that the surface becomes softer during operation. Mechanical properties of the pad material had fluctuating effect on wear rate. The existence of solid particles between pad and disc increasing wear rate and friction coefficient while the mud caused a reduction in wear rate of the pad surface since it acts as a lubricant absorbing the surface heat generated during sliding and reducing the area of contact between pad and disc.

Wear rate obtained experimentally agreed fairly well with that found from empirically obtained equations.

### List of Symbols

A	Apparent area of contact.	H	Hardness.
$A_t$	Real area of contact.	$H_m$	Hardness of the material.
E	Modulus of elasticity.	K	Wear coefficient.



- L Sliding distance of the pad particle relative to the disc.  
 s Sliding distance of abrasive relative to the disc.  
 T Surface temperature of the disc.  
 t Surface temperature of the pad.  
 U Initial velocity.  
 V Wear volume.  
 $V_1$  Wear rate in (mm<sup>3</sup>/m).  
 w Wear rate in (gm/m).  
 W Normal load.  
 $W_1$  Weight of the pad.

#### Greeks

- $\mu$  Coefficient of friction.  
 $\rho$  Density of the friction material.  
 $\tau$  Shear stress.

#### Introduction

The history of the braking of road vehicles is of the same interest to that of the vehicles themselves. The first Benz vehicle was braked by a small brake block applied to a shaft in the transmission. As early as (1900) hand operated spoon or block brakes designed directly on the solid tier were also used. In (1904) the first Daimler car was constructed with a large brake for rear wheels operated by hand-lever.

Front wheel brakes had been used in expensive cars during the First World War. In (1923) most cars were supplied with front-wheel brakes. In (1928) the Lockheed company began to use hydraulically operating brakes<sup>(1)</sup>.

Asbestos-resin based materials were exclusively used to withstand higher brake temperature<sup>(2, 3)</sup>. Metallic particles are always added to modify the coefficient of friction and wear properties of pads<sup>(4)</sup>. The good properties required for friction materials include a high and constant coefficient of friction, good heat conductivity, low wear of both surfaces and low cost<sup>(5, 6, 7)</sup>. Brake components consist of base material copper or iron with a variety of additives, such as (SiO<sub>2</sub> or Al<sub>2</sub>O<sub>3</sub>) to prevent metal transfer.

Graphite is used to prevent friction variety and occasionally inorganic salt to prevent friction reduction at high temperature<sup>(7)</sup>. These materials must not cause excessive wear or grooving on the matting discs, no vibration, pulsation squeal and sensitivity to moisture or water, must also be minimize.

The large amount of energy dissipated during braking can lead to high temperature rise in the brake parts and may cause possible damage to them. To aggravate the problem more, the thermal expansion of the matting brake surfaces can distort the surfaces, so that partial contact occurs, causing excessively high temperature distribution at these contact areas<sup>(8)</sup>. In addition to the damage of the matting surfaces the high temperature will also shorten the life of the seals in the hydraulic systems, and may vaporize the fluid or volatile contaminants in the fluid, bearings may also be affected and loose their lubricants<sup>(9, 10)</sup>.

The main aim of this investigation is to examine experimentally the effects of load, sliding speed, friction material, sliding or braking time, and contaminants (sand or mud) on the wear rate of pads. It is also aimed to find an empirical relationship for the wear rate and friction in pads under the above practical conditions. Actual pads were used in a contaminated environment of sand and mud, to simulate off road conditions.

#### Wear in brakes :-

##### Wear in the pad and the disc

Wear in the pad usually takes the form of adhesive and abrasive wear<sup>(6, 12)</sup>.

Adhesive wear :- When two surfaces are brought into contact, adhesion or bonding across the interface can occur, providing that the two solid surface are cleared all adsorbed oxides and lubricants are removed. The adhesive wear arises when junctions weld together become



broken by relative motion, so wear particles result<sup>(13)</sup>.

It is assumed that the surface asperities are spherical in form (Archard theory), and that the contact areas are circles. It is further assumed that the wear particles will be hemispherical in form with a diameter equal to that of the junction<sup>(13, 14, 15)</sup>.

The wear volume for spherical asperities model<sup>(1, 4, 15, 16)</sup>

$$V = K \frac{W}{3H} \dots\dots\dots (1)$$

and for conical asperities model<sup>(14)</sup>

$$V = K \frac{W \tan \theta}{3H} \dots\dots\dots (2)$$

where  $\theta$  is the base angle of the cone.

**Abrasive wear :-** When dirt or debris becomes entrained in operating tribological system and where it is sufficiently hard, it can produce scoring or abrasion of surfaces in sliding, rolling or rubbing contact<sup>(12)</sup>.

**Two-body abrasion wear :-** The hard surface asperities act rather like cutting tools, removing material from softer surface or two body involved in the interaction like a grinding wheel<sup>(13, 14)</sup>

**Three-body abrasive wear :-** The loose debris of any kind is trapped between sliding surfaces, such as sand or any actual wear particles created by primary process<sup>(17)</sup>. Rabonowicz<sup>(14)</sup> considered a model of abrasive in the form of a cone

$$V = 0.63 \cot \theta \frac{W}{H} \dots\dots\dots (3)$$

but Moore<sup>(18)</sup> considered a model of pyramidal

$$V = \frac{1}{20} \cot \theta \frac{W}{H} \dots\dots\dots (4)$$

Many studies had investigated the wear in the pad of disc brake, most of these studies used pin on disc machine to test the wear in the pad. These studies attempted to find the effect of load, temperature, sliding velocity, surface roughness, braking or sliding time, coefficient of friction, mechanical properties and grain size<sup>(1, 6, 7, 8 ...)</sup>. Some of these studies used the same sample of brake pad and investigated its properties in laboratory<sup>(7, 20, 21)</sup>. It is rather difficult to describe and calculate the process of braking, because of continuous changes of the parameters (speed, load, temperature, mechanical and thermal properties, area of contact ..... etc)<sup>(10, 11)</sup>. Due to this complex phenomenon of wear of pad brake, it is unlikely that there will ever be a global formula in incorporating all the obvious variable to assist the design engineers in carrying out exact calculation<sup>(12, 13)</sup>, so that there are several empirical formulas to calculate, wear, friction and temperature which give result good enough for practical calculations.

In (1985) Ling<sup>(22)</sup> modified Archards wear rate theory which depends on the speed to a new relation depending on temperature

$$w = \frac{KWU}{H} \dots\dots\dots (5)$$

Archard relations

$$w = \frac{KT}{T_s - T} \dots\dots\dots (6)$$

Ling relations

where  $T_s$  is the temperature at which micro hardness first vanishes.

Holm proposed the following formula

$$w = KWU \Delta V \dots\dots\dots (6a)$$

Liu and Rhee<sup>(23)</sup> showed that the wear of many frictional material can be correlated with the equation

$$w = KW^a U^b t^c \dots\dots\dots (7)$$

In the case of three –body abrasive wear

$$w = KW^a U^b t^c \cdot D^n \dots\dots\dots (7a)$$

Where D is the particle size of the sand For constant temperature (t) Puvelasca and Musat<sup>(6)</sup> proposed the following relation

$$w = KW^a U^b \dots\dots\dots (8)$$

using computer program, the value of (K, a, b and c) can be calculated for different materials and cases.

Ho and Peterson<sup>(24)</sup> used the following relation

$$w = K \frac{T}{T_m - T} \dots\dots\dots (9)$$

where  $T_m$  = melting temperature of the pad.

Pavelescu and Musat<sup>(6)</sup>, Ho and Peterson<sup>(24)</sup> proposed the following relation to estimate the temperature

$$T = KW^a t^b \dots\dots\dots (10)$$

The above mentioned equations are empirical formulas, during this work mathematical equations have been developed to calculate and investigate the wear rate and coefficient of friction for the cases of two body and three body abrasive wear.

Considering a conical single asperity its maximum height is ( $h_m$ ). The model asperity in this case is that of the metallic disc, and it is assumed to penetrate the frictional pad at a depth of ( $h$ ) from its surface.

$$\varepsilon = \text{relative approach} = h/h_m$$

$$\eta = \frac{A_t}{A} \quad (\eta < 1)$$

$$\eta = b \cdot \varepsilon^{\nu^1} = \frac{A_t}{A}$$

$$A_t = bA\varepsilon^{\nu^1} \dots\dots\dots (11)$$

Where  $b, \nu^1$  are constant depending on the surface finish. The values of ( $b$ ) ranges from (0 to 10),  $\nu^1$  from (2 to 3) and  $c$  from (0 to 1)<sup>13</sup>.

Consider a light load causing a penetration nearly equal to ( $dh$ ), so that the volume ( $dv$ ) will be

$$dv = A_t \cdot dh \dots\dots\dots (12)$$

$$dh = h_m \cdot d\varepsilon \dots\dots\dots (13)$$

total volume,

$$v = \int_0^{\varepsilon} dv = \int_0^{\varepsilon} A_t \cdot dh \dots\dots (14)$$

substitute equations (11) and (13) into (14)

$$v = \int_0^{\varepsilon} A \cdot b \cdot \varepsilon^{\nu^1} \cdot h_m \cdot d\varepsilon$$

$$v = \frac{A \cdot b \cdot h_m \cdot \varepsilon^{\nu^1+1}}{\nu^1+1} \dots\dots\dots (15)$$

Substitute equation (11) into (15) to get

$$v = \frac{A_t \cdot h_m \cdot \varepsilon}{\nu^1+1} \dots\dots\dots (16)$$

but  $H = \frac{W}{At}$

therefore, equation (16) becomes

$$\nu^1 = \frac{W}{H} \cdot \frac{h_m \cdot \varepsilon}{(1+\nu^1) \cdot L}$$

$$w = \frac{W}{H} \cdot \frac{h_m \cdot \varepsilon}{(1+\nu^1) \cdot L} \cdot \rho \dots (17)$$

where ( $w$ ) is the wear rate in (gm/m) ,  $h_m$  can be obtained from appendix (c)

Equation (17) is the mathematical model for two-body abrasive wear. The developed equations for three body abrasive wear and coefficient of friction between disc and pad are

$$v = \frac{c \cdot s \cdot W (1 + \frac{H_m K_s}{2E})^2}{H_m \cdot \pi \cdot \tan \theta} \dots (18)$$

Equation (18) must be modified to suit the practical conditions.

1. displacement (S) of the abrasive relative to the metal is unknown, but it can be related by

$$S = K_o \cdot L$$

Where :-

- $K_o$  = constant from the experiment  
 = 0.5 when the sliding surfaces have the same hardness as the abrasive  
 = 0.95 when the surface is soft
2. The proportionality coefficient (c) includes many factors, five components at dry friction and six components at lubricated condition

$$c = \frac{k_1 \cdot k_2 \cdot k_3 \cdot k_4}{k_5 \cdot k_6} \dots (19)$$

For this investigation the values of the parameters in equation (18) for the sand and mud samples were substituted, the final equations are

- a. Dry case

$$v_1 = 1.137 \times 10^{-5} \frac{k_1 w \left(1 + 9.35 \left(\frac{H_m}{E}\right)\right)^2}{H_m} \dots (20)$$

- b. For mud

$$v_1 = 0.762 \times 10^{-5} \frac{k_1 w \left(1 + 9.35 \left(\frac{H_m}{E}\right)\right)^2}{H_m} \dots (21)$$

The coefficient of friction seems to be dependent on some parameters like normal load, density, surface velocity, and area of contact

$$\mu = f(w \cdot \rho \cdot u \cdot A) \dots (22)$$

by using dimensional analysis, and solving the algebraic equations simultaneously

$$\mu = k \left( \frac{\rho \cdot u^2 \cdot A}{w} \right) \dots (23)$$

The complete derivations of the above mentioned equations are reported in reference (26).

### Experimental work :-

#### Equipments

The layout of the test rig is shown in fig. (A). Briefly it consists of a three-phase 380/50 HZ A-C motor, 15 HP, 22 amperes and 2920 rpm maximum speed, used to drive the gear box.

The gear box has three speeds and one reversed speed and is driven by a v-belt. A bevel gear of reduction (1/3.33) is connected to the gear box through a universal joint to transmit the motion to the disc which is 90° inclined. A (120 x 65 x 1.5 cm) rigid table of 120cm height made of steel plate used to carry the brake device and the disc.

#### Brake device

The brake system consists of a disc of (240mm) outer diameter, (130mm) inner diameter and (9.8mm) thickness. Two pads of surface area (33.18cm<sup>3</sup>) were used. A gauge pressure having a range of (0 to 60 atm) used to measure the fluid pressure. An electrical balance having rang of (0.01gm to 1000gm) used to weigh the pad before and after the experiment.

#### Temperature measurements

To measure the surface temperature of the rotating disc a (NiCr, NiAL) trailing thermocouple having a range of (-50 c° to 900 c°) was used. The sensor was placed vertically on the brake



disc soon after braking. The sensor was connected to a digital thermometer.

To measure the surface temperature of the pad, three (NiCr, NiAl) thermocouple located (1mm) underneath the pad's surface were used. The thermocouples were connected to a digital read-out of 8-channel equipment.

A tachometer of different ranges was connected to the shaft for monitoring the rotational velocity of the disc rotor.

Three commercial pads of different origin were selected for this investigation. The tests were performed in the following environmental conditions

1. Two-body sliding
2. Three-body sliding using sand
3. Three-body sliding with water using mud.

When the brake is active, the pressure increases on the disc pads and wear will occur on the pad only due to difference in hardness of the disc and pad.

The weight of the pad before and after the test was measured, besides time of braking, pressure of the brake fluid, surface temperature of the disc and the pad. Rotational velocity of the disc, sand particle size and mud concentration were all measured also.

A simple apparatus was designed to measure the friction force (Appendix B). Surface content tests were performed using a metallurgical microscope with a magnification power of (100), which gave the composition of the pad samples, used in the investigation (Appendix A). The pads were photographed before and after testing by magnifying the pad surface under the microscope to about (100) times.

Hardness and bending tests were used to establish the mechanical properties of the pads. The thermal conductivity was measured in the laboratory and density of the pad material was calculated by using a simple method depending on the volume and weight.

The surface roughness of the disc and the pads was checked before and after

testing using a Talysurf (Appendix C). the particle size of the sand was established by using sieving analysis and checked by the microscope after magnifying a sand particle about (25) times. The hardness of the sand was taken to be  $(800 \text{ kg/mm}^2)^{(25)}$ .

### Experimental Results :-

The extensive experimental results indicated the behavior of wear rate of pads under a wide variety of conditions such as :-

#### The Effect of Load .

Figures (1), (2) and (3) represent the relation between the wear rate and the load applied on the pad. The figures show a linear relation between the wear rate and the applied load. The figures show also that the applied loads cannot be lowered to smaller values. This due to :-

1. Reducing the load to smaller values reduces the braking effect (sliding only).
2. Applying light load, the wear rate will be very small and cannot be measured.

In general, the pads can be classified according to their wear rate as belw.

The wear rate of ( $T_u$ ) pad > wear rate of ( $I_y$ ) pad > wear rate of ( $I_R$ ) pad for the same load and velocity. These figures show that the wear rate increased when sliding time increased.

Figures (4, 5, 6 and 7) show the effect of sliding time on the wear rate. The result shown have been obtained by applying light loads on the pad for certain time (longer than the normal case). These figures show that the wear rate becomes higher in this case, because sliding has longer time than braking time causing higher surface temperature. From the wear rate point of view, the pads can be classified as mentioned before.

The effect of sand particles of different size and concentration on the wear rate can be shown in figures (8, 9, 10, 11, 12 and 13). The wear rate is

higher surface temperature. From the wear rate point of view, the pads can be classified as mentioned before.

The effect of sand particles of different size and concentration on the wear rate can be shown in figures (8, 9, 10, 11, 12 and 13). The wear rate is considerable more comparing with the normal case. The higher the concentration and larger the size of the sand particles, the higher is the wear rate. Increasing the sliding time will increase the wear rate as can be seen in figures (14, 15, and 16). Figure (14) shows that sliding occurs with the application of light loads have a great effect on the wear rate of the pad, while for the heavier loads the sliding time seems to have no effect on wear rate. It is clear that by increasing sliding time the temperature of the surface of the pads increased, reducing the shear stress at pads surface, so that the asperities will be easy cut. This case can be noticed when light load applied at the pads, while applying heavy load the solid particles of the sand embedded in the pad material, compressing the asperities, causing an increase in the area of contact and reduction in ploughing force.

Figures (17), (18) and (19) show the effect of the mud between the pad and the disc on the wear rate. The temperature rise of the pad surface will be lower than in the other cases, because the mud acts as a lubricant (coolant) absorbs part of the surface temperature so that the wear rate becomes less than in ordinary cases.

#### **The effect of mechanical and physical properties on the wear rate.**

Experimentally noticed that the wear rate of the ( $I_y$ ) pad is more than the ( $I_R$ ) pad, although the ( $I_y$ ) pad is harder than the ( $I_R$ ) pad. Checking the surface temperature of both types of pads during sliding operations found they are not equal. That could be the reason.

The pads with higher Young's modulus of elasticity ( $E$ ) show lower wear rate than that with lower modulus of elasticity ( $E$ ). Since the material of higher Young's modulus of elasticity has higher internal resistance to the plastic deformation, because of the forces combined the molecules increases the surface energy which prevent the penetration of the peaks of the hard surface to that of the lower hardness.

#### **The effect of grain size.**

The larger the particle size of the solid particles between the pad and the disc surfaces, the higher is the wear rate, since the larger particles cause deep ploughing on the pad surface.

#### **Friction Results :-**

The results obtained from the experimented tests carried out to study the parameters affected the friction of the brake pads can be seen in figures (20, 21, 22, 23, 24, and 25).

Figures (20, 21, and 22) represent the variation of the friction coefficient between the pad and the disc with load for different speeds. It can be deduced that there is slight reduction in friction coefficient by increasing the load and the speed. The surface temperature of the pad increases with increasing the sliding speed which reduces the shear force, hence reduced friction force.

Figures (23, 24, and 25) show the effect of the sand particles between the pad and the disc on the friction coefficient. The solid particle causes an increase in the coefficient of friction since these particles cause higher ploughing than in the normal case, hence increasing the friction force, which is a resultant of three component of forces namely the adhesive force, the ploughing force and the shear force. The figures also show that the coefficient of friction was affected by the grain size of



the solid particles, since it becomes higher for larger particle size.

Regarding the theoretically derived equations (17, 20, 21) figures (26, 27 and 28) represent a comparison between the theoretical and experimental values of the wear rate. There is slight difference between the theoretical and experimental results. The wear rate obtained experimentally is affected by simultaneous conditions like surface roughness, surface temperature, hardness .... etc, while in the theoretically derived equations these parameters have not been considered.

To calculate the wear rate, from equations (20, and 21), using the same constants used by Ling and Wang<sup>(19)</sup>, the theoretical results proved to be near to the experimental results, when using ( $k_1 = 0.25$  to  $0.33$  this means that an acceptable amount of the solid particles existed between the pad and the disc. When  $k_1 = 1$ , this means that the solid particles filled the region between the disc and the pad, while if  $k_1 = 0$ , this means that there is no solid particles between the pad and the disc). In solving equation (18), many values for ( $k_0, k_1, k_2, k_3, k_4, k_5, k_6$ ) were examined. The wear rate calculated theoretically from this equation and that obtained experimentally were nearly the same when the following constant were used,  $\theta = 80^\circ$ ,  $k_0 = 0.5$  to  $0.6$ ,  $k_1 = 0.20$  to  $0.35$ ,  $k_2 = 1$  to  $1.3$ ,  $k_3 = 0.6$  to  $0.8$ ,  $k_4 = 0.42$  to  $0.67$ ,  $k_5 = 1$ ,  $k_6 = 1$  to  $4$ .

The Archard equation (equation 5) was solved and the suitable value of the wear coefficient ( $k$ ) has been found to be ( $3 \times 10^{-5}$ ) for ordinary braking.

The ( $I_R$ ) pad has the lower value of the wear coefficient than the other.

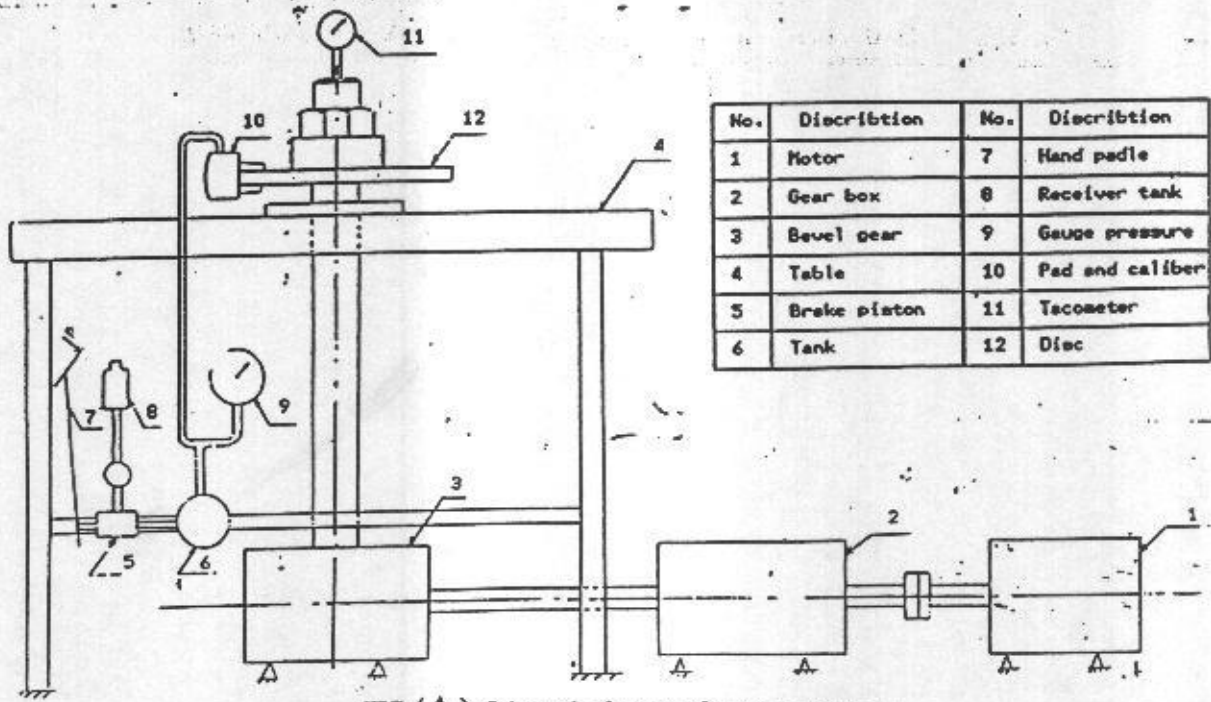
From the test results using numerical procedure, equations (7)(7a) also equation (23) have been solved to find the constant ( $a, b, c$  and  $n$ ). All the results obtained are presented in Appendix (D) in form of tables. The results obtained from solving the mathematically derived equations are presented in Appendix (E)

## Appendix B

### Friction force measurement

A simple apparatus was designed to measure the friction force. It consisted of an elastic member attached to an adjustable screw carried by a rigid holder which was fixed to the table. The pad was fixed to the end of the elastic member; the deflection of the elastic member was measured by a dial gauge. The system was calibrated by applying different loads; this gave a linear relation between the deflection of the elastic member and the applied load.





No.	Description	No.	Description
1	Motor	7	Hand paddle
2	Gear box	8	Receiver tank
3	Bevel gear	9	Gauge pressure
4	Table	10	Pad and caliber
5	Brake piston	11	Tacometer
6	Tank	12	Disc

FIG (A) Schematic layout of wear apparatus .

APPENDIX (A)

TABLE OF SPECIFICATIONS OF PAD MATERIAL.

sample	surface contains	$F \times 10^8$ kg/m <sup>2</sup>	$E \times 10^8$ HV/m <sup>2</sup>	HRB	K u/m. <sup>2</sup> c
1Y	Fe, Cu, Zn < Ba < Sb and Sr, Al, Mg and Si in a little amount.	2.100	2.985	75.142	0.80
1R.	Cu < Sb < Ba and Zn, Al, Fe trace .large amount of asbeste.	1.870	2.623	36.500	0.85
TU.	Mg ,Fe , Zn and Ni, Si. Large amount of rubber.	1.747	2.270	39.000	0.65

APPENDIX (C)

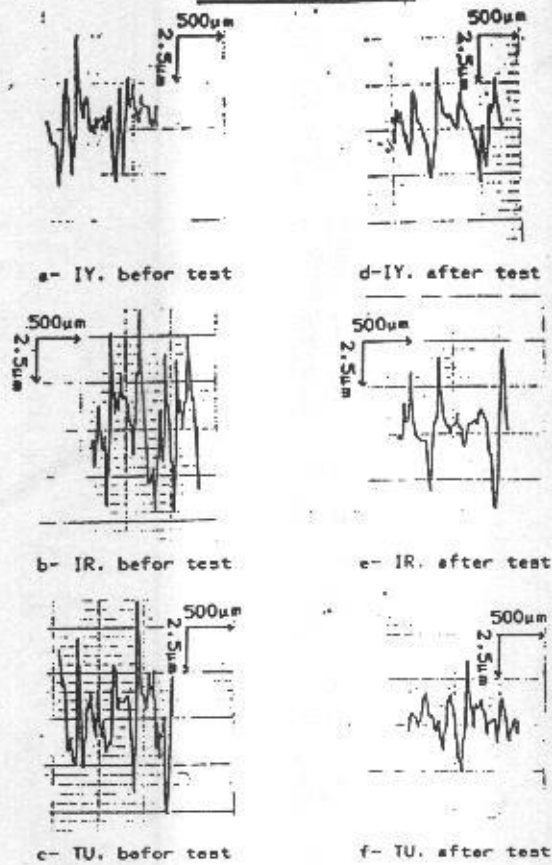


FIG. (C-1) | Surface roughness of pads (a,b,c,befor test and d,e,f,after fifteen brakes).

APPENDIX (C)

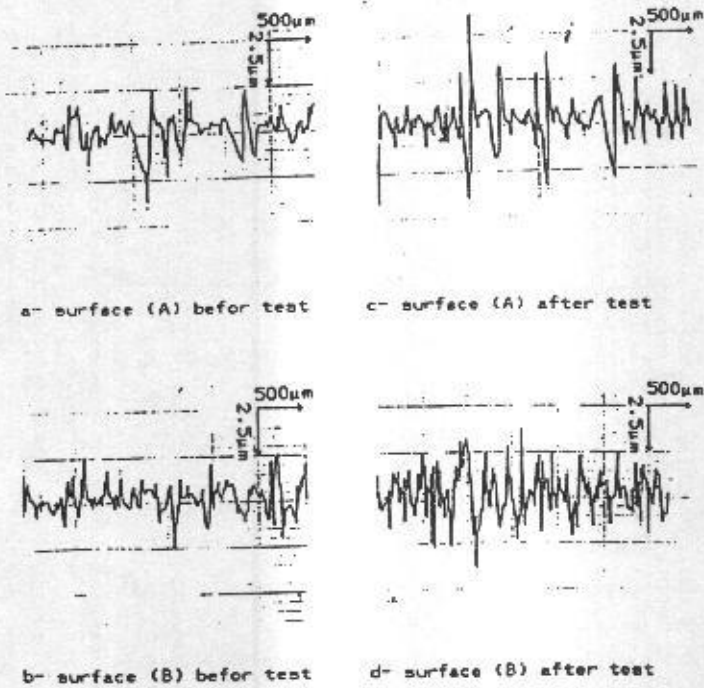


FIG. (C-2) | Surface roughness of disc (a,b,befor test and c, d,after fifteen brakes).



APPENDIX (D)  
TABLE (D-1) : WEAR AND TEMPERATURE EQUATION.

WEAR				TEMPERATURE			
CASE 1: BRAKING WITH OUT CONTAMINANTS BETWEEN THE SURFACES							
TYPE	$\delta$	$\alpha$	$\beta$	$\epsilon$	$\theta$	$\phi$	$\psi$
IY.	$4.899E-7$	.4345	.9424	-.7880		.6090	.4370
IR.	$14.29E-7$	.9030	.7479	-.7820		1.120	.1184
IU.	$40.84E-7$	.4361	.8520	-1.277		1.963	.1917
CASE 2: BRAKING WITH SAND BETWEEN THE SURFACES							
IY.	$7.304E-5$	.3070	-1.081	-.8230	.8118	.8717	.4110
IR.	$112.3E-5$	.4230	.2025	-.8440	.7752	1.700	.1670
IU.	$21.84E-5$	.4770	.6E-4	-.2160	.2260	3.681	.3250
CASE 3: SLIDING WITH H2O BETWEEN THE SURFACES							
IY.	$4.679E-5$	.5180	-.224			1.260	.8972
IR.	$5.189E-5$	.3390	-.271			1.3770	.8680
IU.	$3.629E-5$	.5130	-.940			1.0820	.8277

TABLE (D-2) : COEFFICIENT OF FRICTION EQUATION.

TYPE	FRICTION (WITHOUT CONTAMINANTS)		FRICTION (WITH SAND)	
	$k$	$f$	$k$	$f$
IY.	.4518	.1652	.7723	.2040
IR.	.4140	.8472	.8643	.1141
IU.	.4790	-.8387	.8427	.8715

APPENDIX (E)

TABLE (E-1): WEAR COEFFICIENT (k) ((equation (5))).

TYPE	WITH OUT CONTAMINANTS	WITH SAND	WITH H2O
IY.	$.75 \times 10^{-4}$	$.42 \times 10^{-4}$	$4.50 \times 10^{-4}$
IR.	$.30 \times 10^{-4}$	$.27 \times 10^{-4}$	$3.15 \times 10^{-4}$
IU.	$.58 \times 10^{-4}$	$.39 \times 10^{-4}$	$3.82 \times 10^{-4}$

TABLE (E-2): THE VALUE OF K1 ((equation (20))).

TYPE	BRAKING WITH SAND	SLIDING WITH SAND
IY.	0.29	0.35
IR.	0.25	0.29
IU.	0.27	0.31

TABLE (E-3): THE VALUE OF CONSTANT IN EQUATIONE (18): & (19):

TYPE	$K_0$	$K_1$	$K_2$	$K_3$	$K_4$	$K_5$	$K_6$
IY.	0.68	0.33	1.24	0.76	0.47	1	1.20
IR.	0.49	0.22	1.05	0.63	0.64	1	3.45
IU.	0.59	0.29	1.16	0.71	0.55	1	2.68

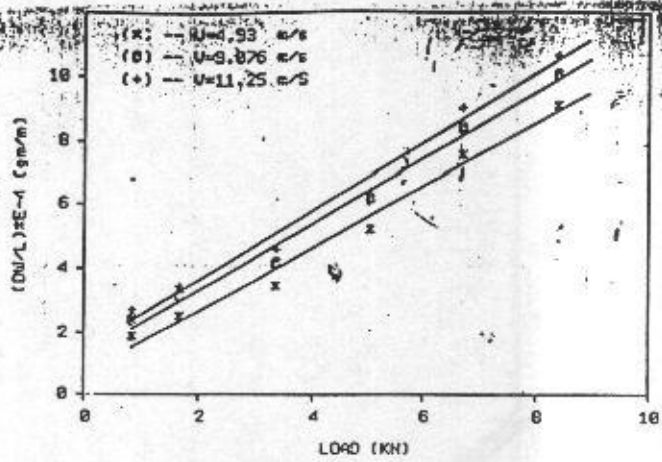


FIG (1): Wear Rate vs. Load For Iy. Pad (dry case)

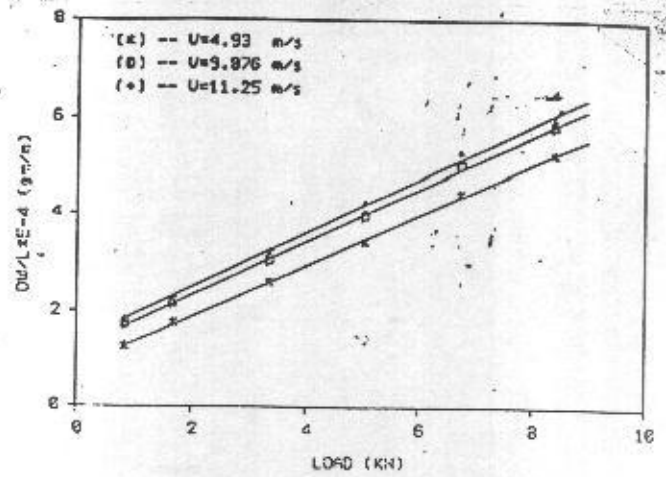


FIG (2): Wear Rate vs. Load For Ir. Pad (dry case)

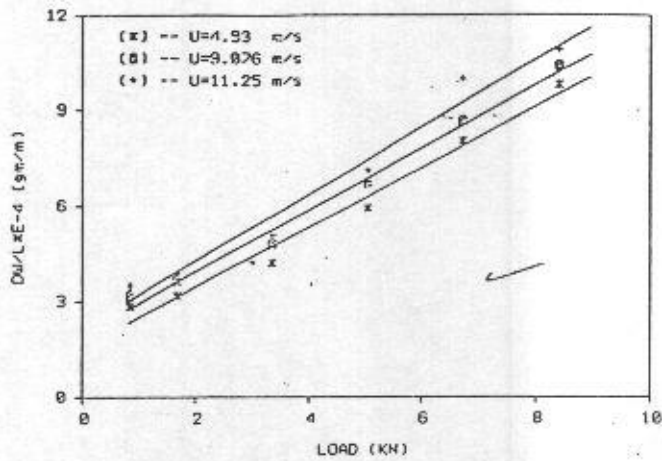


FIG (3): Wear Rate vs. Load For Tu. Pad (dry case)

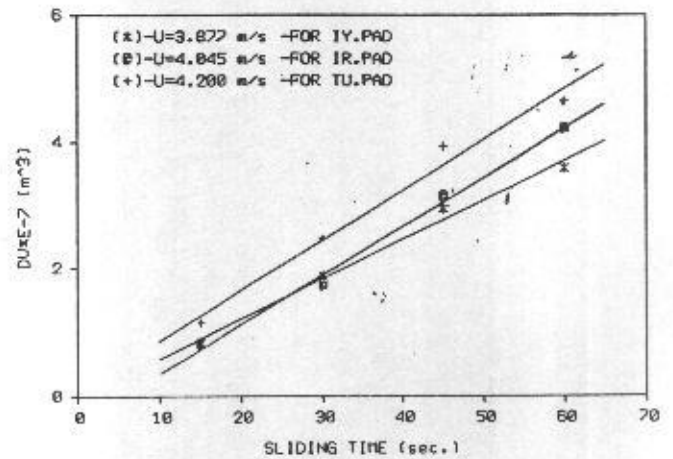


FIG (4): Wear vs. Time At Constant Load = 0.84 KN (sliding case)

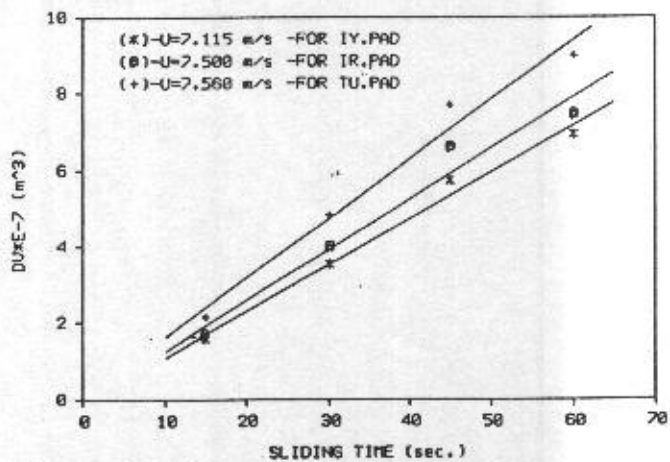


FIG (5): Wear vs. Time At Constant Load = 0.84 KN (sliding case)

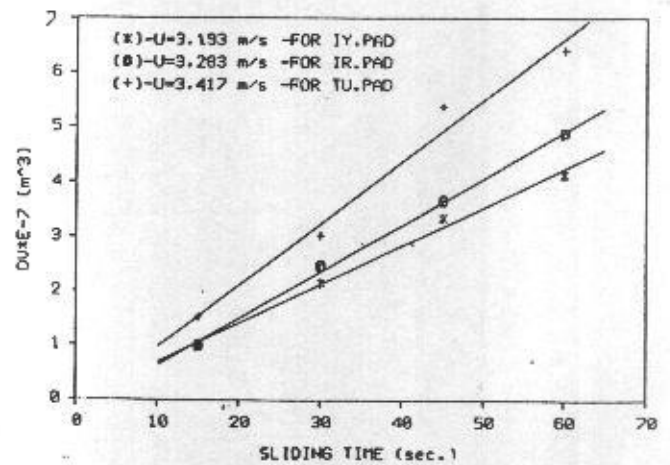


FIG (6): Wear vs. Time At Constant Load = 1.68 KN (sliding case)



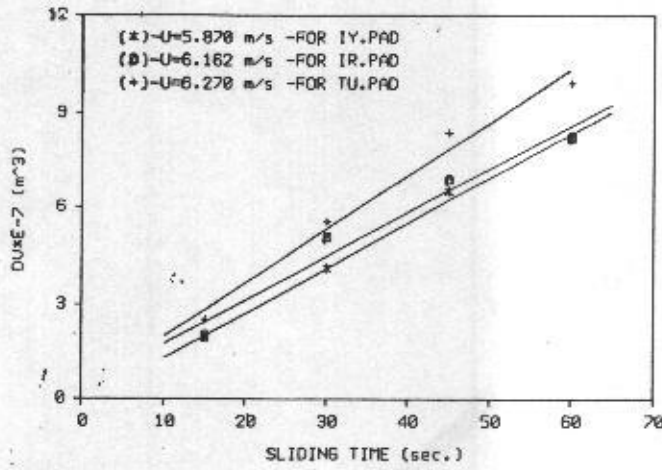


FIG (7): Wear Us, Time (Load =1.68 KN) (sliding case)

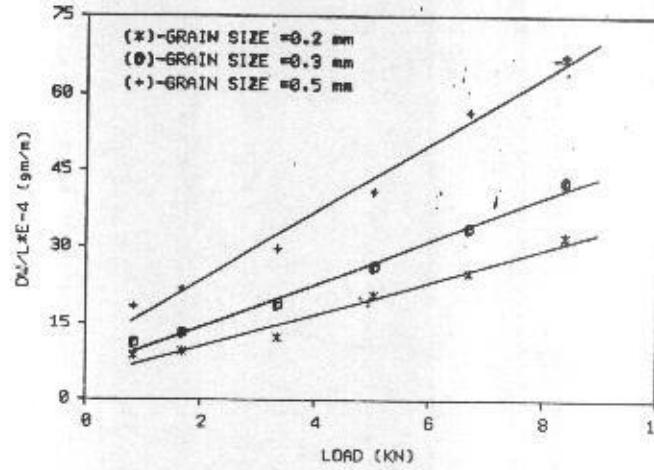


FIG (8): Wear Rate Us, Load For IY. Pad At U=4.93 m/s (when used sand)

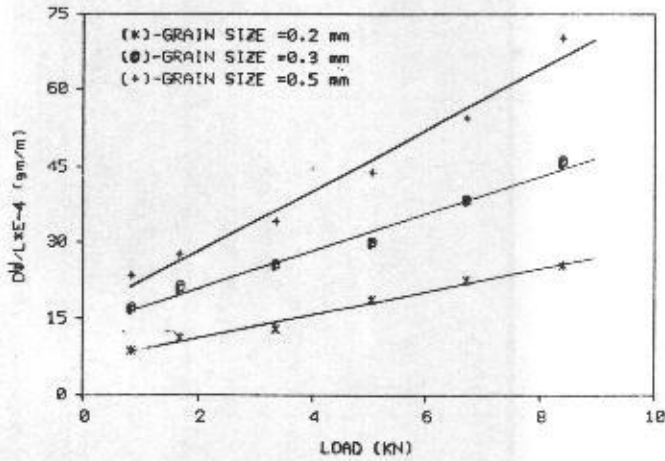


FIG (9): Wear Rate Us, Load For IY. Pad At U=9.076 m/s (when used sand)

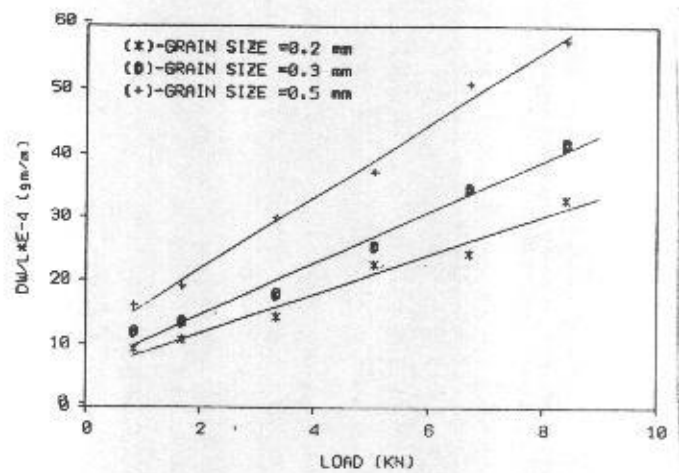


FIG (10): Wear Rate Us, Load For TU. Pad At U=4.93 m/s (when used sand)

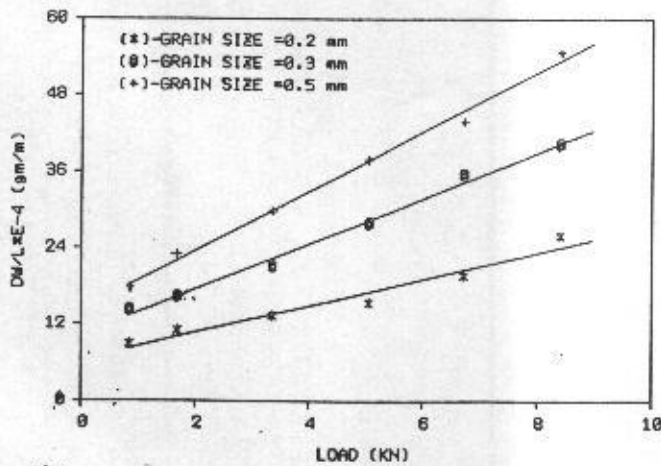


FIG (11): Wear Rate Us, Load For TU. Pad At U=9.076 m/s (when used sand)

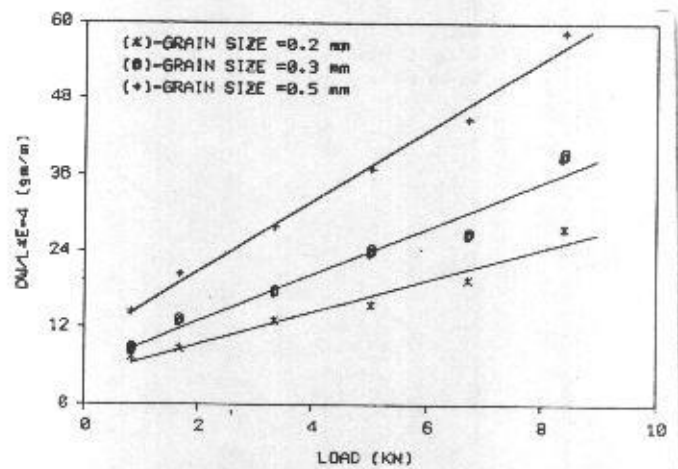


FIG (12): Wear Rate Us, Load For IR. Pad at U=4.93 m/s (when used sand)

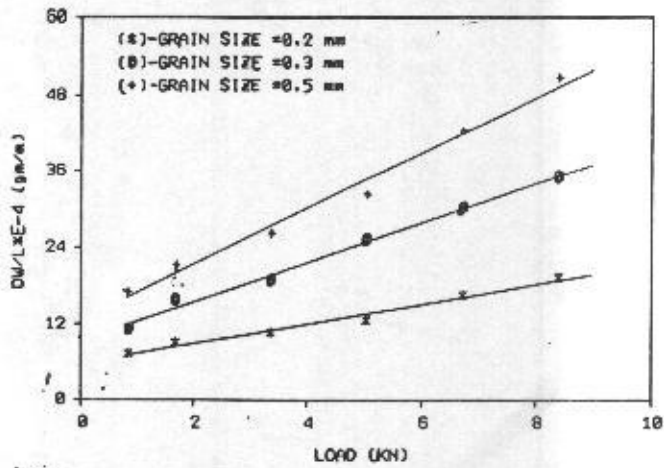


FIG (13): Wear Rate Us. Load For IR. Pad At  $U_o=9.876$  m/s (When used sand)

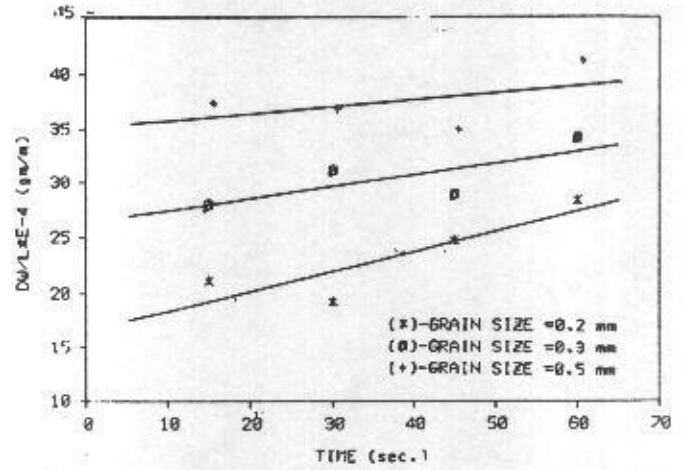


FIG (14): Wear Rate Us. Time For IV. Pad At ( Load =0.335 kn and  $U_o=4.93$  m/s ) For sliding case .

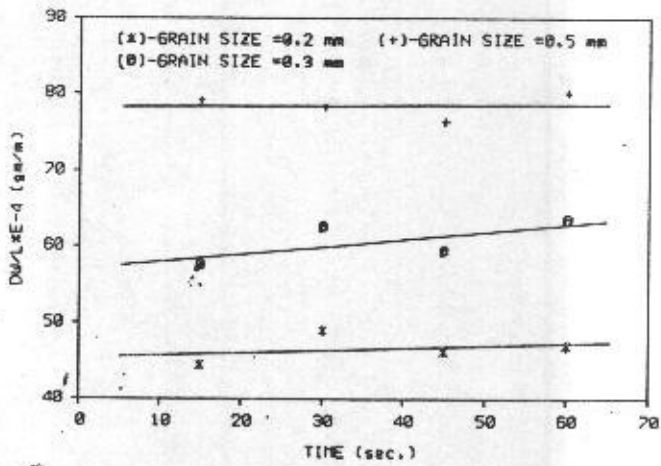


FIG (15): Wear Rate Us. Time For IV. Pad AT ( Load =0.872 kn and  $U_o=4.93$  m/s ) For sliding case .

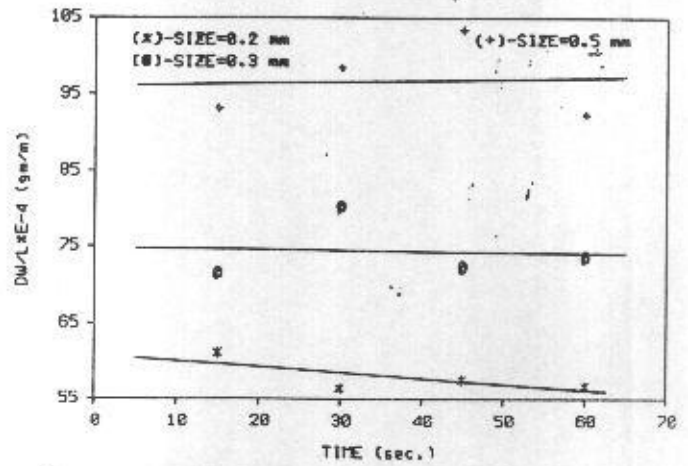


FIG (16): Wear Rate Us. Time For IV. Pad AT ( Load=1 kn and  $U_o=4.93$  m/s ) For sliding case .

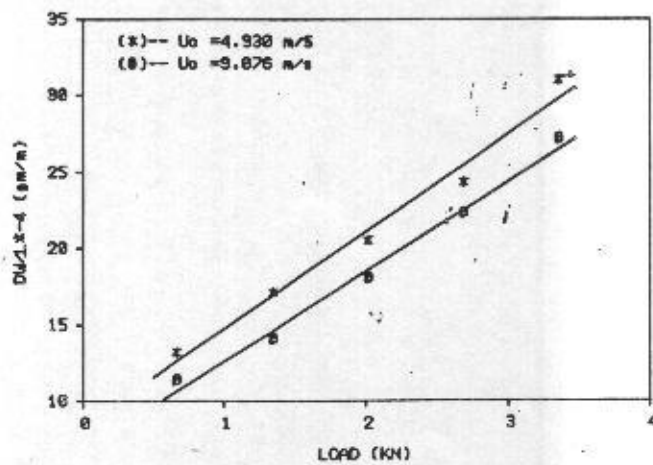


FIG (17): Wear Rate Us. Load For IV. Pad At Constant Time =5 min. (when used mud)

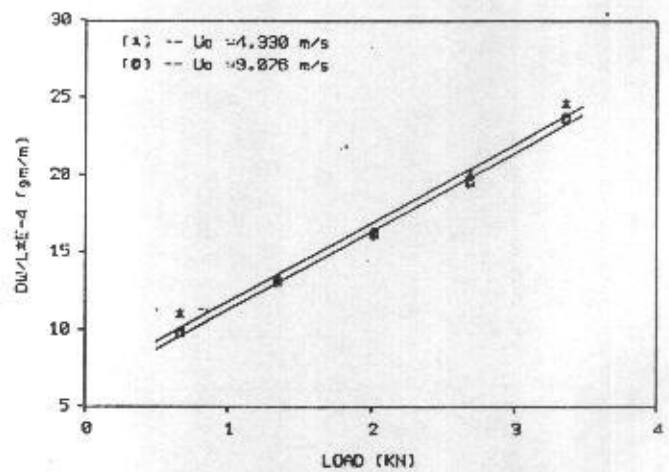


FIG (18): Wear Rate Us. Load For TU. Pad At Constant Time =5 min. (when used mud).



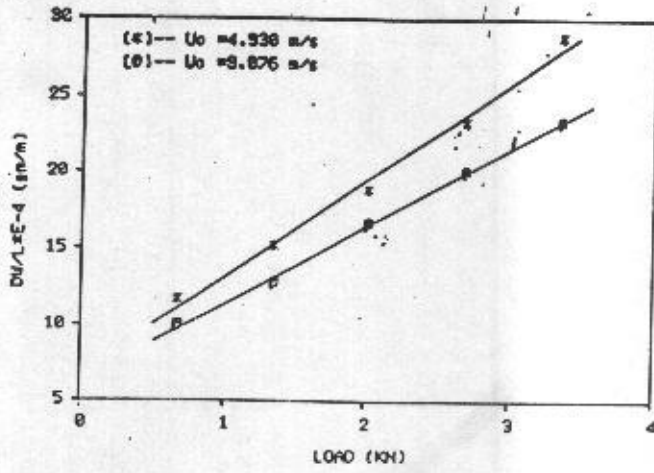


FIG (19): Wear Rate vs. Load For IR. Pad At Constant Time = 5 min. (When used mud)

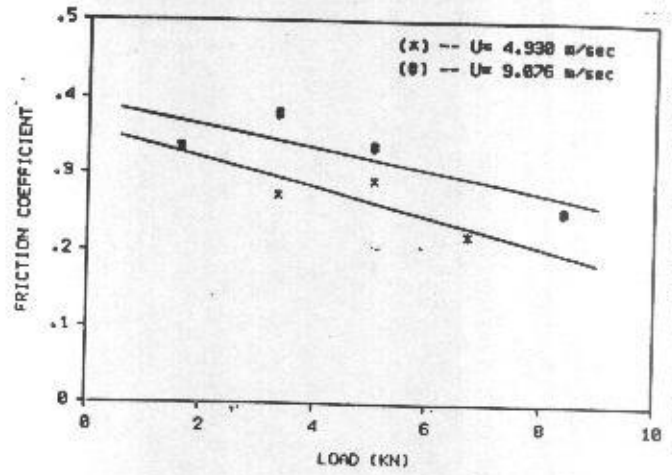


FIG (20): Friction coefficient vs. load for IV. pad .

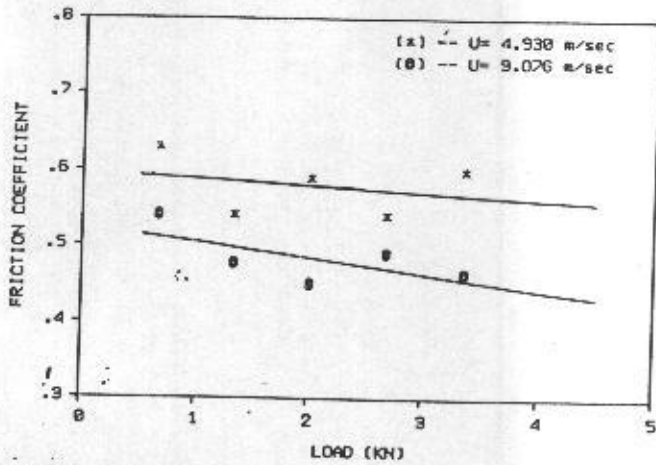


FIG (21): Friction coefficient vs. load for TU. pad .

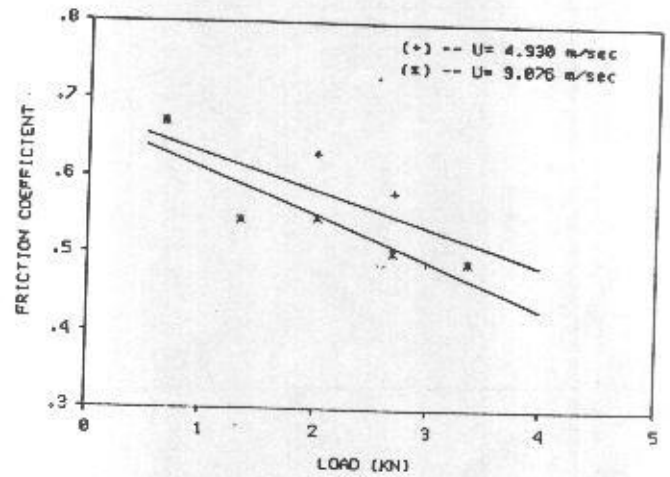


FIG (22): Friction coefficient vs. load for IR. pad .

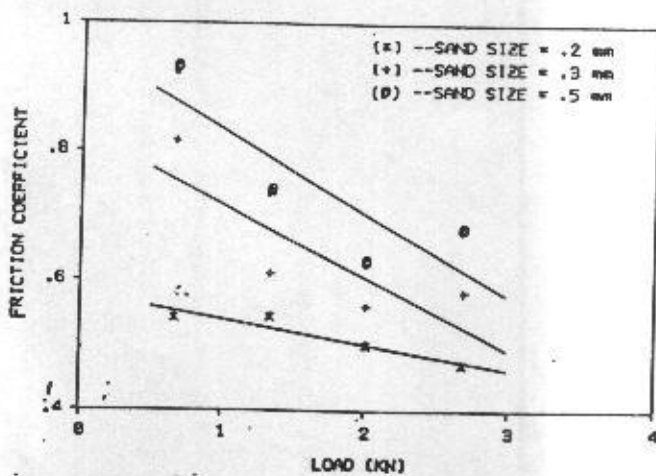


FIG (23): Friction coefficient vs. Load for IV. pad with sand.

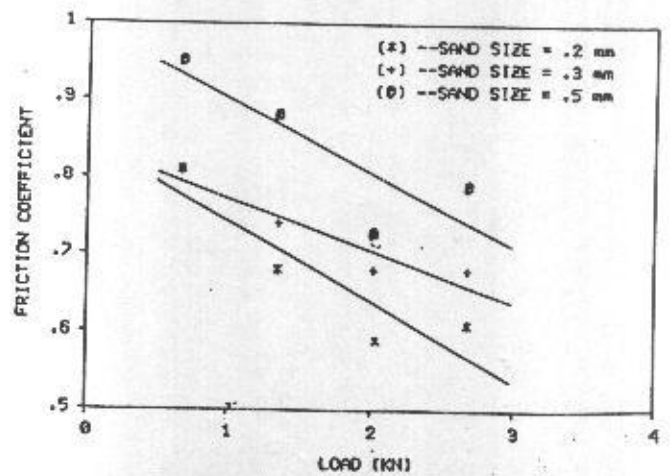


FIG (24): Friction coefficient vs. load for TU. pad with sand .

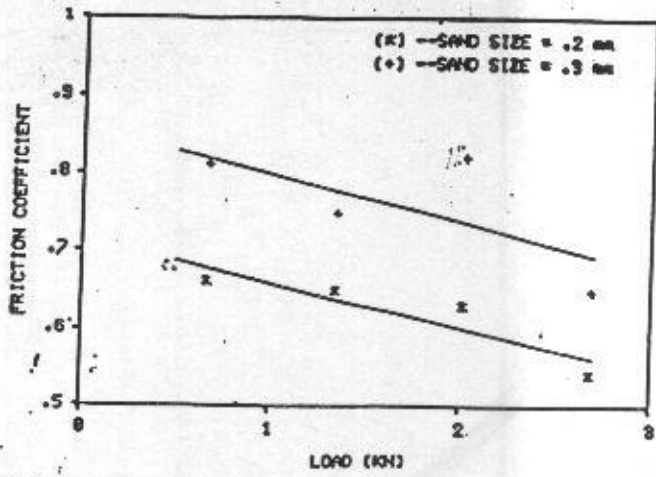


FIG (25): Friction coefficient vs. load for IR. pad with sand.

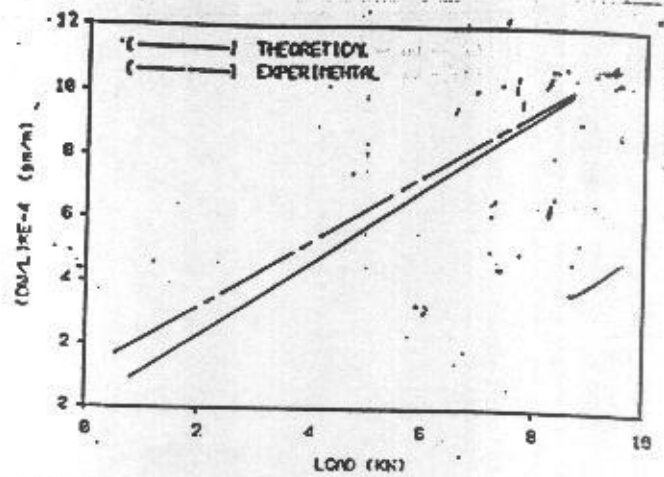


FIG (26): Wear Rate vs. Load For IV. Pad.

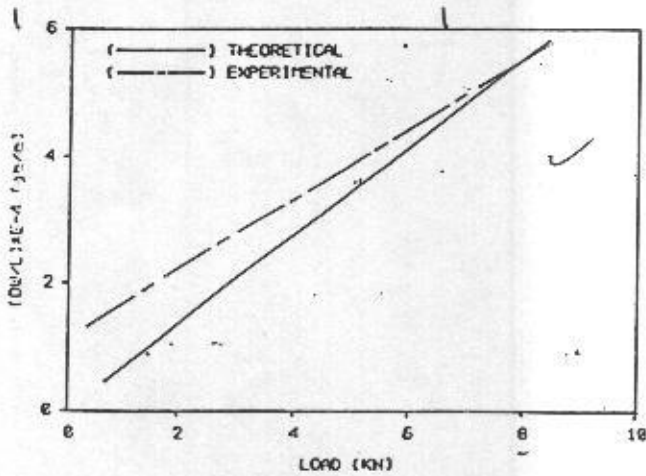


FIG (27): Wear Rate vs. Load For IR. Pad .

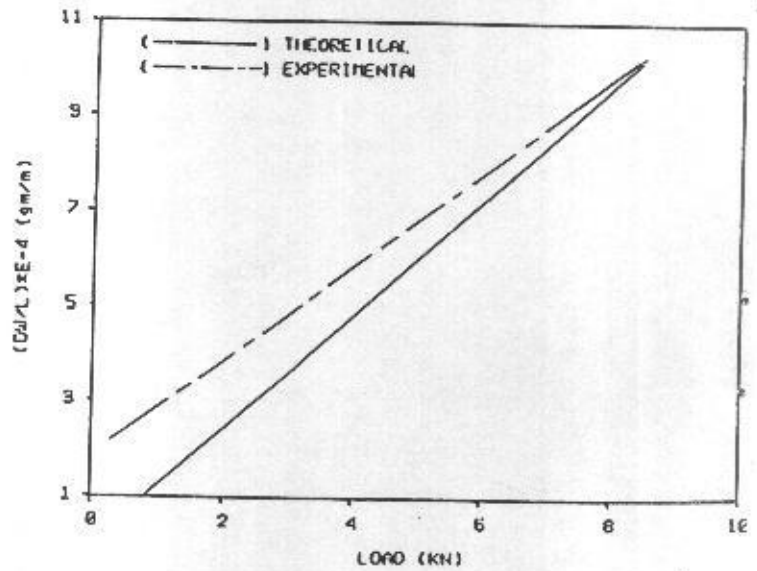


FIG (28): Wear Rate vs. Load For TU. Pad .



## REFERENCES

1. K. Tanaka, "Fundamental studies on the brake friction of resin-based friction materials" *Wear*, V23, pp. 349-365 (1973).
2. T.P. Newcomb and M. EL-Sherbeni, "Liquid-cooled disc brakes", *Wear*, V34, pp. 311-317, (1975).
3. B. Weaving, "Environmental consideration in the selection of friction materials for rail application", *I.Mech. E.*, C172/79, pp. 159-166, (1979).
4. T. Liu and S.K. Rhee, "High temperature wear of semi-metallic disc brake pads", *wear*, V46, pp. 213-218, (1978).
5. P.H.S. Tsang, M.G. Jaka and S.K. Rhee, "Comparison of chase and inertial brake dynamometer testing of automotive friction materials" *Wear*, V103, pp. 217-232, (1985).
6. D. Pavelcsu and M. Musat, "Some relations for determining the wear of composite brake materials" *Wear*, V27, pp. 73-91, (1974).
7. T.L. Ho M.B. Peterson and F.F. Ling, "Effect of friction heating on brake materials" *Wear*, V30, pp. 73-91, (1974).
8. T.A. Dow, "Thermo-elastic effects in brakes" *Wear* V59, pp. 213-221, (1980).
9. T.P. Newcomb, "Energy dissipated during braking" *Wear*, V59, pp. 401-407, (1980).
10. T.P. Newcomb and R.T. Spurr, "Temperature as a criterion of failure in brakes and clutches" *First European Tribology congress*, London, C2 66/73, pp. 71-77, (1973).
11. T.A. Libach and S.K. Rhee, "Micro-structural changes in semi-metallic disc brake pads" *Wear*, V46, pp. 203-212, (1978).
12. A. Chichinadze and A. Ginzburg, "Theoretical and experimental investigation of friction under braking", *First European Tribology Congress*, London, C2 71/73, pp. 101-107, (1973).
13. A.D. Sarkar, "Friction and wear" J. W. Arrowsmith, Bristol, (1980).
14. E. Rabinowicz, "Friction and wear of materials" Wiley, New York, (1965).
15. B. Pugh, "Friction and wear", Butterworths, London, (1973).
16. B.J. Chapman and A.A.M. Rizkallah-Ellis, "Effect of the surface finish of brake rotors on the performance of brakes", *Wear*, V57, pp. 345-356, (1979).
17. J. Halling, "introduction to tribology" Wykeman, London, (1976)
18. D.F. Moore, "Principles and applications of tribology" Pergamon, Oxford, (1975).
19. y. Ling Wang and ZI. Shan Wang, "An analysis of influence of plastic indentation on three-body abrasive wear of metals" *Wear*, V122, pp. 123-133, (1988).
20. P.J. Blau, "Interpolations of the friction and wear brake-in behavior of metals in sliding contact" *Wear*, V71, pp. 29, (1981).
21. M.G. Jaka, "Physical and chemical changes of organic disc pads in service" *Wear of materials*, ASME, United engineering center, New Yourk, (1977).
22. F.F. Ling, "A reassessment of the wear of copper-based brake material at elevated temperatures" *Wear*, V102, pp. 43-49, (1985)
23. T. Liu and S.K. Rhee, "High temperature wear of asbestos-reinforced friction materials" *Wear*, V37, pp. 291-297, (1967).
24. T.L. Ho and M.B. Peterson, "Wear formulation for air-craft brake material sliding against steel" *Wear*, V43, pp. 199-210, (1977).
25. H.J. Mohammed "An investigation of the stuges in a process of adhesive and obrasive mechanical wear" M.Sc. thesis, university of Baghda, (1980).
26. M.H. Jassim "An investigation into the friction and wear behavior of disc brake material", M.Sc. thesis, university of Baghdad.

## دراسة التآكل والاحتكاك الحاصل لوسادة الموقف الامامي للسيارة الصغيرة

د.عزيز العلوي      د.البييرت يوسف      منير عبدالحسين جاسم  
(خلال فترة اعداد هذا البحث كان المؤلفون في قسم الهندسة الميكانيكية - كلية الهندسة - جامعة بغداد).

### الخلاصة

يتضمن هذا البحث دراسة عملية ونظرية لمعدل التآكل والاحتكاك الحاصل لوسادة الموقف الامامي للسيارة الصغيرة. اشتملت الدراسة العملية على اختبار ثلاث وسائد موقف مختلفة المنشأ تحت سرع وأحمال وظروف بيئية مختلفة على جهاز بسيط تم اعداده لهذا الغرض. تركز البحث على دراسة مقدار التآكل الناتج عن عملية الحك كونه الأكثر وضوحاً عند تآكل وسادة الموقف. أختبرت بعض النماذج مع وجود مادة الرمل أو الطين بين القرص والوسادة تحت ظروف تشغيل مختلفة من سرع وأحمال وزمن توقف. تطلبت الدراسة تحديد بعض الخواص الميكانيكية لوسادة الموقف قيد الاختبار ( الصلادة، معامل المرونة، حمل الانهيار اثناء الحناية ). كذلك تم تحديد معامل التوصيل الحراري وفحص نعومة السطح للاستفادة منها في مقارنة السطح قبل وبعد التشغيل. لوحظ من خلال التجارب أن للسرعة تأثير محدود على معدل التآكل ولكن تأثيرها أوضح على معامل الاحتكاك ، اما الحرارة فلها دور رئيسي على مقدار التآكل والاحتكاك فزيادتها تقلل من معامل الاحتكاك وتزيد من معدل التآكل. لم يكن لنعومة السطح دور واضح على مقدار التآكل حيث لوحظ تغير نعومة السطح بعد أول عملية تشغيل. أما تأثير الخواص الميكانيكية فكان تأثيرها متباين على مقدار التآكل. أوضحت الدراسة إن توجد مواد صلبة مثل الرمل بين الوسادة والقرص أدى الى زيادة سريعة في مقدار التآكل ومعامل الاحتكاك ، اما وجود المادة الطينية فقد أدت الى تقليل معدل التآكل (حيث كان للطين دور المزييت وساعد بامتصاص قسم من الحرارة المتولدة). لوحظ إن معدل التآكل المستحصل عمليا في حالة تطابق جيد مع ذلك المحسوب من المعادلات التطبيقية.